A New Process for Al_2O_3 Production from Low-Grade Diasporic Bauxite Based on Reactive Silica Dissolution and Stabilization in NaOH-$NaAl(OH)_4$ Media

Jiayu Ma, Zhibao Li, and Qinggui Xiao

Key Laboratory of Green Process and Engineering, National Engineering Laboratory for Hydrometallurgical Cleaner Production Technology, Institute of Process Engineering, Chinese Academy of Sciences, Beijing 100190, PR China

DOI 10.1002/aic.12722

Published online July 28, 2011 in Wiley Online Library (wileyonlinelibrary.com).

A new process of Al_2O_3 production from low-grade diasporic bauxite based on the reactive silica dissolution and stabilization in concentrated NaOH-$NaAl(OH)_4$ solutions is proposed and proved feasible. NaOH and Al_2O_3 concentrations and leaching temperature were found to be the main factors affecting the leaching process of reactive silica. The A/S *(mass ratio of Al_2O_3/SiO_2) of diasporic bauxite was enhanced from 5.4 to 15 by reactive silica removal under the optimum operation conditions. Two obvious steps control the whole leaching process of reactive silica in NaOH-$NaAl(OH)_4$ media: reactive silica dissolution and desilication products (DSPs) precipitation. The kinetics data of two controlling steps fit a shrinking core model based on the calculation of OH^- activity with the aid of OLI platform and an empirical kinetic model well, respectively. Apparent activation energies of reactive silica leaching in the temperature range from 80 to 110 °C are 101.91 and 58.65 kJ mol^{-1} for the two steps, respectively. The stabilization mechanism of reactive silica in concentrated NaOH-$NaAl(OH)_4$ solution was also elucidated based on the complexation of aluminum-bearing species and the calculation of supersaturation to DSP. It was found that the concentration of OH^- sharply decreases due to the formation of $Al(OH)_4^-$ species with increasing aluminum concentration, suppressing greatly DSP precipitation. This proposed process paves the way for Al_2O_3 production from low-grade diasporic bauxite with high-reactive silica content.* © 2011 American Institute of Chemical Engineers *AIChE J,* 58: 2180–2191, 2012

Keywords: reactive silica, kinetic modeling, Bayer process, stabilization, dissolution, precipitation

Introduction

Bauxite is the most important raw materials in alumina/aluminum production. It is composed of one or more aluminum hydroxide minerals, including primarily gibbsite [$Al(OH)_3$], boehmite[γ-AlO(OH)] and diaspore [α-AlO(OH)].[1] There are also other compounds in bauxite such as kaolinite [$Al_2Si_2O_5(OH)_4$], quartz [SiO_2], hematite [Fe_2O_3], goethite [FeO(OH)], rutile/anatase [TiO_2], and other impurities in minor or trace amounts.[1] Currently, the Bayer process (Figure 1) is the most common hydrometallurgical method for the production of pure alumina.[2] In the Bayer process, ground bauxite is digested with caustic solution in steam-agitated autoclaves at high temperatures. After digesting, the resulting sodium aluminate solution is separated from the mud residue (mixtures of alumina, silica, calcium oxide, iron oxide, titanium oxide, and so on) and cooled before entering the precipitation tanks of the crystallization section. The solution is also seeded with recycled fine alumina trihydrate, which results in additional precipitation. The larger particles are recovered, washed, and calcined to make the alumina product. The spent liquor is returned to the digestion step where it is contacted with further bauxite.[3]

Unlike bauxite ores found in other countries, more than 80% of the bauxite in China is of diasporic characteristics with low ratios of alumina to silica (A/S: 4-6).[4] It cannot be processed economically through the Bayer process due to its low grade.[5,6] Therefore, several processes such as sintering, [7,8] and modified Bayer processes such as those including floating[9–12] and lime,[13–16] have been developed and applied to produce alumina from low-grade bauxite ore in the alumina refineries of China. However, those processes have encountered many problems. For example, the sintering process is commonly associated with high costs and high energy consumption.[17] The flotation Bayer process requires large amount of reagents that are added into the process and generates tailings totaling some 25% by weight of the initial bauxite ores, which cannot be easily reused due to their complicated composition and structure.[18] The lime Bayer process cannot effectively reduce scaling throughout the remainder of the plant and is not sufficiently effective for processing low-grade bauxite ores with $A/S < 5$.[3,19] Therefore, an economic method for processing low-grade diasporic bauxite in China, especially for ores with $A/S < 5$, does not currently exist.

Correspondence concerning this article should be addressed to Z. Li at zhibaoli@mail.ipe.ac.cn.

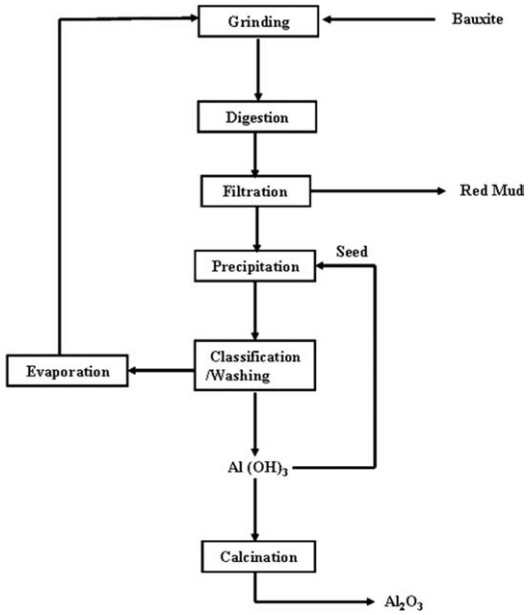

Figure 1. Illustrative flowsheet of the traditional Bayer process.

In lime Bayer process,[20,21] lime is usually added in order to reduce soda losses[22,23] during predesilication prior to digestion. The primary purpose of predesilication is to ensure that conversion of reactive silica to desilication products (DSPs) is complete so that pregnant liquor from digestion contains a minimum amount of dissolved silica. However, the predesilication efficiency is low (<50%) and reprecipitation of DSP on plant surfaces will cause scale build-up in the process.[24,25]

Reversely, transferring a large proportion of the reactive silica in bauxite directly into solution for a period sufficient to enable a solid/liquid separation is a good idea. In this new design, the dissolution of at least a substantial part of the reactive silica from the bauxite and the stabilization of dissolved silica in solution for a period of time (or stability) sufficient to effect a solid/liquid separation is the key. Therefore, it is necessary to investigate the leaching kinetics of the reactive silica from the bauxite in NaOH-$NaAl(OH)_4$ media.

The leaching mechanism and kinetics of silica compounds have been described in the Bayer process literature. Kaolinite, which is usually the predominant source of reactive silica in bauxite, dissolves quickly in Bayer liquor. Once a certain level of silica in solution is reached, silica reacts with alumina and soda to form DSP.[26] Roach and White[27] found that kaolinite dissolution in synthetic sodium aluminate solution is promoted mainly by high free caustic concentration and high temperature. The degree of crystallinity or nature of the kaolin (kaolinite or halloysite) has also been reported to influence silica dissolution rate. Banvolghi et al.[28] proposed a mechanism whereby kaolinite transforms to sodium aluminum silicate without significant dissolution in the digestion of high silica bauxite (>5% SiO_2, A/S = 6.9) in caustic solution at 80–130 °C. Using scanning electron microscopic (SEM) and Infrared Spectroscopy (IR) techniques, the authors found that OH^- and Na^+ ions react with gibbsite, but the Si—O bonds resist attack and transform gradually to sodalite. Sodium hydroxide concentration was cited as the driving force for kaolinite dissolution. The kaolinite reaction has also been described as occurring in three stages at 100°C.[29] In the first 50 min, kaolinite dissolves gradually, increasing solution silica levels. At about 50 min, precipitation of a DSP begins. After 135 min, the concentration of DSP reached a constant level. Buhl et al.[30] followed the hydrothermal transformation of kaolinite to sodalite in pure sodium hydroxide using nuclear magnetic resonance. The rate of transformation was enhanced by increasing temperature (80–200°C) and by the presence of carbonate in solution.

Quartz is less susceptible to caustic attack than kaolinite and only begins to react above 180°C.[22] Oku and Yamada[31] studied the dissolution rate of quartz in the digestion of monohydrate bauxite at 180–240°C. The dissolution of quartz was found to be first order with respect to quartz surface area, controlled by the chemical reaction of OH^- at the surface of the quartz and an activation energy of 82 kJ mol^{-1} calculated for the reaction. The presence of dissolved aluminum ions has been reported to inhibit quartz dissolution.[32]

Recently, the removal of reactive silica from gibbsite in NaOH-$NaAl(OH)_4$ solution was studied by Hollitt et al.[3] They found that a liquor having a high caustic and alumina concentration can allow rapid solubilization of reactive silica and stabilize a high level of silica in solution for a period of time sufficient to effect a solid/liquid separation.

Most of the previous studies have been focused on the leaching of pure silica compounds (kaolinite and quartz) or reactive silica from gibbsite. However to date, very limited studies involving the reactive silica leaching from diasporic bauxite have been reported. Moreover, an overall leaching kinetic model incorporating the behaviors of reactive silica dissolution and DSP precipitation has not yet been presented.

In this article, the leaching of the reactive silica from low-grade diasporic bauxite in NaOH–$NaAl(OH)_4$ media was studied. More specifically, the experimental parameters affecting the leaching of reactive silica, including NaOH concentration, mean particle size of the diasporic bauxite, Al_2O_3 concentration, leaching temperature, and time were investigated in detail. A classical shrinking core model was applied to determine the controlling step, and an empirical kinetic model for DSP precipitation has been applied to fit the experimental data in two stages, respectively. Then, the kinetic parameters and activation energies were obtained. Moreover, the mechanism of reactive silica stabilization in concentrated NaOH-$NaAl(OH)_4$ solution was elucidated with help of the calculation of activity and supersaturation. Finally, a new process for Al_2O_3 production from low-grade diasporic bauxite based on the reactive silica dissolution and stabilization in NaOH–$NaAl(OH)_4$ media is proposed and is experimentally proven.

Experimental

Materials

The diasporic bauxite used in this study is from KAIMAN Alumina Company (China). The chemical composition of the diasporic bauxite is listed in Table 1. Analytically pure $Al(OH)_3$, $Na_2SiO_3 \cdot 9H_2O$, and CaO were all supplied by Sinopharm Chemical Reagent Co. Ltd. with minimum purities of 98.5, 97.5, and 98.0%, respectively. NaOH (98.0%) was supplied by Chemical Company of Beijing. The starting aluminate solution with the required content of alkali and alumina was prepared by dissolving sodium hydroxide and aluminum hydroxide in double distilled water (conductivity < 0.1 μS cm^{-1}) and heating to 110°C with agitation for 30 min till all the aluminum hydroxide had been dissolved.

Table 1. Mineralogical Composition of Bauxite from KAIMAN Alumina Company (China)

Chemical Composition	wt.%	Mineralogical Composition	wt.%	
Al	32.9	Al	In gibbsiteand	2.0
Si	5.4		Boehmite	
Fe	4.4		Diaspore	23.5
Ti	2.4		Kaolinite	7.1
Ca	0.29		Hematite	0.3
K	0.85		Total	32.9
		Si	In kaolinite	5.0
			Quartz	0.4
			Total	5.4
		Fe	In goethite	1.2
			Hematite	3.2
			Total	4.4

Experimental apparatus

The 1-L mixed tank reactor used in this study was made from glass, as shown in Figure 2. The reactor was heated by circulating oil from a thermostat batch within ±0.5°C and stirred with a Teflon impeller driven by a variable speed motor under autocontrolled agitation.

Measurement of silica stability in NaOH-NaAl(OH)$_4$ solution

Silica stability experiments were conducted in the same reactor. A total of 400 mL of the prepared NaOH solution or sodium aluminate solution with the required content of alkali and alumina was heated to 90°C with circulating oil. On attainment of 90°C, addition of 100 mL of 50 g L^{-1} SiO_2 sodium silicate solution at once and stirring at 300 rpm were simultaneously started. Samples of 5 mL were taken at prearranged time intervals, immediately filtered with a 0.22-μm membrane filter, and the liquor was analyzed for silica. The residues were then filtered, washed three times, dried at 80°C for about 10 h, and analyzed by X-ray diffraction (XRD).

Measurement of reactive silica leaching kinetics

The kinetics experiments of reactive silica leaching in diasporic bauxite were conducted as follows. A total of 500 mL of the prepared NaOH solution with various concentration levels of sodium aluminate was introduced into the same reactor, which was heated by oil bath, set to the desired temperature, for at least 1 h to equilibrate the temperature of the solution. Then a certain amount of dry raw bauxite with the particle size of 50~125 μm was rapidly added into the reactor, whist stirring at 300 rpm. Suspension samples of 5 mL were withdrawn at prescribed times, immediately filtered with a 0.22-μm membrane filter, and the separated liquor was recovered for analysis. Finally, the residues were filtered, washed three times, dried at 80°C for about 10 h, and analyzed to determine their chemical and mineralogical compositions.

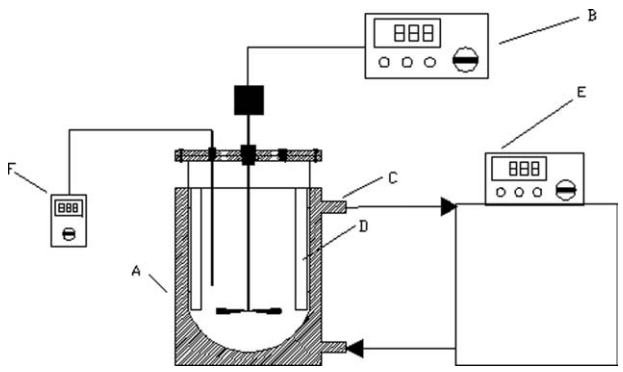

Figure 2. The diagram of experimental apparatus.

A, heating jacket; B, impeller controller; C, oil circulator; D, 4 baffles attached to the lid; E, band heater; F, thermometer.

Chemical analysis and characterization

The Na_2O concentration of the sodium aluminate solution was determined by volumetric analysis with HCl solution and phenolphthalein as the indicator. The Al_2O_3 concentration was analyzed by the chelating titration method with ethylenediaminetetraacetic acid (EDTA), using Xylenol orange as the indicator. The silica concentration in the solution was determined by ultraviolet–visible spectrophotometer (UNICOUV-2000). Polarizing microscopy (DMRX, LEICA, Germany) was used to identify the mineralogical phases of the treated bauxite. X-ray fluorescence (XRF) was used to determine the chemical composition of the raw bauxite, the treated bauxite, red mud, and Al_2O_3 obtained. The solid Al_2O_3 products obtained were further examined using powder XRD and SEM (JEOL-JSM-6700F). Powder XRD (X'Pert PRO MPD, PANalytical, Almelo, The Netherlands) patterns were recorded on a diffractometer (using Cu Kα radiation) operating at 40 kV/30 mA. A scanning rate of 0.02°/s was applied to record the patterns in the 2θ angle range of 5°– 90°.

Chemistry of Aqueous Aluminum and Silica in NaOH Solution

Aluminum in sodium hydroxide solutions occurs as various kinds of species, such as $Al(OH)_4^-$, $AlOH^{2+}$, $Al(OH)^{2+}$, $Al(OH)_3^0$, Al^{3+}, and so on.[33–36] The speciation diagram of aluminum ions in NaOH solution was constructed with the help of the OLI platform and is presented in Figure 3. As can be seen, the tetrahedral $Al(OH)_4^-$ ion is the predominant species in alkaline solutions with pH higher than 10, which is consistent with the results reported in the literatures.[36,37]

In the Bayer process, reactive silica is first dissolved in the liquor and then the dissolved silica precipitates as DSP.[20,38] Therefore, the whole leaching process of reactive silica in NaOH-NaAl(OH)$_4$ media can be subdivided into two parallel and simultaneous reactions: the dissolution of reactive silica and DSP precipitation.[26]

In the reactive silica dissolution step, the reactive silica (kaolinite) of the bauxite is attacked by caustic soda to form silicon and aluminum bearing species.

$$Al_2O_3 \cdot 2SiO_2 \cdot 2H_2O(s) + 6OH^- + H_2O \longleftrightarrow 2Al(OH)_4^- + 2H_2SiO_4^{2-} \quad (1)$$

In the DSP precipitation step, silicon species is reacted with aluminum species to form DSP.

$$8Na^+ + 2OH^- + 6Al^{3+} + 6SiO_2(aq) + 14H_2O \longleftrightarrow Na_8Si_6Al_6O_{24}(OH)_2(H_2O)_2(s) + 24H^+ \quad (2)$$

The supersaturation (S) of the solution with respect to DSP was defined as the ratio of the activity products divided by the thermodynamic equilibrium constant (also called the

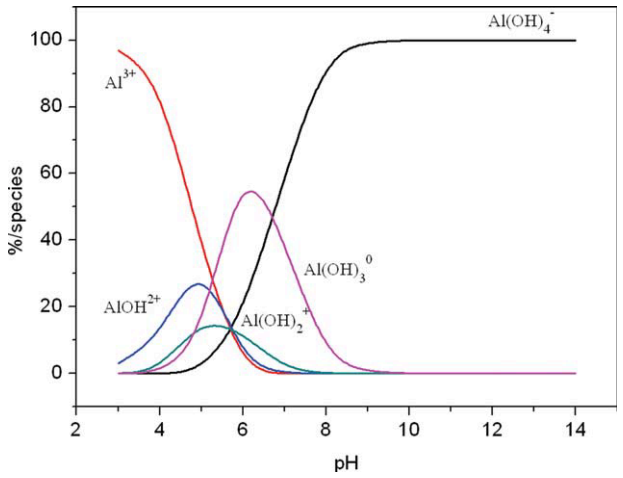

Figure 3. Speciation diagram of aluminum ions in NaOH solution at 25°C and 1 atm.

[Color figure can be viewed in the online issue, which is available at wileyonlinelibrary.com.]

solubility product constant, K_{SP}, in solid–liquid equilibria) of DSP

$$S = \frac{(a_{Na^+})^8(a_{OH^-})^2(a_{Al^{3+}})^6(a_{SiO_2})^6(a_w)^{14}}{K_{sp}(a_{H^+})^{24}} = \frac{\left[(m_{Na^+})^8(m_{OH^-})^2(m_{Al^{3+}})^6(m_{SiO_2})^6\right] \times \left[(\gamma_{Na^+})^8(\gamma_{OH^-})^2(\gamma_{Al^{3+}})^6(\gamma_{SiO_2})^6\right] \times (a_w)^{14}}{K_{sp}(m_{H^+})^{24}(\gamma_{H^+})^{24}} \quad (3)$$

where a_{Na^+}, a_{OH^-}, $a_{Al^{3+}}$, a_{SiO_2}, and a_{H^+} are the activities (mol kg^{-1}) of Na^+, OH^-, Al^{3+}, SiO_2, and H^+, respectively, in solution; m_{Na^+}, m_{OH^-}, $m_{Al^{3+}}$, m_{SiO_2}, and m_{H^+} are the corresponding concentrations in molality (mol kg^{-1}); γ_{Na^+}, γ_{OH^-}, $\gamma_{Al^{3+}}$, γ_{SiO_2}, and γ_{H^+} are the ion activity coefficients; a_w is the activity of water.

Finally, the chemistry of the $Al_2O_3{\cdot}2SiO_2{\cdot}2H_2O$-NaOH-$NaAl(OH)_4$-$H_2O$ system can be presented by partial dissolution of $Al_2O_3{\cdot}2SiO_2{\cdot}2H_2O$ and association (speciation) of ionic species as below.

$$H_2O \longleftrightarrow H^+ + OH^- \quad (4)$$

$$Al^{3+} + OH^- \longleftrightarrow AlOH^{2+} \quad (5)$$

$$AlOH^{2+} + OH^- \longleftrightarrow Al(OH)_2^+ \quad (6)$$

$$Al(OH)_2^+ + OH^- \longleftrightarrow Al(OH)_3(aq) \quad (7)$$

$$Al(OH)_3(aq) + OH^- \longleftrightarrow Al(OH)_4^- \quad (8)$$

$$H^+ + H_2SiO_4^{2-} \longleftrightarrow H_3SiO_4^- \quad (9)$$

$$Al_2O_3 \cdot 2SiO_2 \cdot 2H_2O(s) + 6OH^- + H_2O \longleftrightarrow 2Al(OH)_4^- + 2H_2SiO_4^{2-} \quad (1)$$

$$8Na^+ + 2OH^- + 6Al^{3+} + 6SiO_2(aq) + 14H_2O \longleftrightarrow Na_8Si_6Al_6O_{24}(OH)_2(H_2O)_2(s) + 24H^+ \quad (2)$$

Kinetic Modeling Framework

The kinetics of reactive silica dissolution

The Shrinking Core Kinetic Model Based On Activity. In the reactive silica dissolution step, solid kaolinite reacts with OH^- ions (from the NaOH-$NaAl(OH)_4$ solution) and produces a soluble silicate complex. In this work, the kinetic model used to describe the concentration of dissolved silica with time takes into account reactive silica dissolution as an irreversible, first-order reaction with respect to OH^- activity. According to the shrinking nonporous particles model,[39] the rate is assumed to be proportional to the surface area of the kaolinite particles A, as follows:

$$\frac{dC_{SiO_2}}{dt} = kAa_{OH^-} \quad (10)$$

where C_{SiO_2} is the dissolved silica concentration (mol L^{-1}). k is the kinetic rate constant. The surface area of the particles, which are assumed to be spherical, is:

$$A = N4\pi r^2 \quad (11)$$

where N is the number of particles and r is the average particle radius. It is observed that the particle radius changes along the reaction time. This can be related to the kaolinite concentration (moles of kaolinite/volume of solution), C_{kaolin}, by taking into account the variation of the volume of the particles:

$$\frac{C^0_{kaolin} - C_{kaolin}}{C^0_{kaolin}} = \frac{\frac{4}{3}\pi r_0^3 - \frac{4}{3}r^3}{\frac{4}{3}\pi r_0^3} = 1 = \frac{r^3}{r_0^3} \quad (12)$$

where r_0 is the initial particle radius. As 2 mol of silica goes into solution for each mole of dissolved kaolinite,[40] the difference $C^0_{kaolin} - C_{kaolin}$ is half the amount of dissolved silica C_{SiO_2}, and Eq. 12 can be rewritten as below:

$$\frac{r}{r_0} = \left(1 - \frac{C_{SiO_2}}{2C^0_{kaolin}}\right)^{1/3} \quad (13)$$

One should observe that $C_{SiO_2}/2C^0_{kaolin}$ can be regarded as the conversion of the kaolinite. Substituting Eq. 11 and Eq. 13 into Eq. 10, the following equation can be obtained:

$$\frac{dC_{SiO_2}}{dt} = kN4r_0^2\left(1 - \frac{C_{SiO_2}}{2C^0_{kaolin}}\right)^{2/3} a_{OH^-} \quad (14)$$

The size of the kaolinite particles used in all the experiments was always the same, which means that r_0 is a constant value. Also, the mass of kaolinite was constant in all experiments, meaning that the number of particles was approximately the same. All the constants appearing in Eq. 14 were lumped together with the kinetic constant k_1. So, Eq. 14 can be rewritten as:

$$\frac{dC_{SiO_2}}{dt} = k_1\left(1 - \frac{C_{SiO_2}}{2C^0_{kaolin}}\right)^{2/3} a_{OH^-} \quad (15)$$

The activity of OH^- ions in solution is given by

$$a_{OH^-} = m_{OH^-}\gamma_{OH^-} \quad (16)$$

In the NaOH-NaAl(OH)$_4$-H$_2$O system, the relation between m_{OH^-} and C_{OH^-} is given by

$$m_{OH^-} = \frac{C_{OH^-}}{\rho - 0.001 \sum C_i MW_i} \quad (17)$$

where ρ is the solution density in g mL^{-1}, and MW_i is the molar mass of the species i in g mol^{-1}. C_{OH^-} was calculated according to the following equation:

$$C_{OH^-} = \left(C^0_{OH^-} - 3C_{SiO_2} - 2C^0_{Al_2O_3}\right) \quad (18)$$

where C_{OH}-^{0} and C^0_{Al2O3} are the initial concentrations (mol L^{-1}) of OH^- and Al_2O_3, respectively.

Activity Coefficient of OH^- Ion. It is clear from Eq. 16 that determination of the activity of OH^- ion in solution requires the knowledge of the OH^- ion activity coefficient. There are several types of coefficient models that may be used in this context.[41,42] However, the Bromley–Zemaitis activity coefficient model[42] developed by Bromley[43] and empirically modified by Zemaitis[41] is one of the models used by the OLI software. This model has been successfully used for electrolytes with concentrations of 0–30 M at 0–200°C; hence, it is appropriate for calculating the OH^- ion activity coefficient in the NaOH-NaAl(OH)$_4$-H$_2$O systems after validation. The Bromley–Zemaitis activity coefficient model for the case of cation i in a multicomponent electrolyte solution is expressed as follows:

$$\log \gamma_i = \frac{-AZ_i^2\sqrt{I}}{1+\sqrt{I}} + \sum_j \left[\frac{(0.06 + 0.6B_{ij})|Z_iZ_j|}{\left(1 + \frac{1.5I}{|Z_iZ_j|}\right)^2} + B_{ij} + C_{ij}I + D_{ij}I^2 \right] \times \left(\frac{|Z_i| + |Z_j|}{2}\right)^2 m_j \quad (19)$$

where j indicates all anions in solution, A is the Debye–Huckel parameter, I is the ionic strength of the solution, B, C, and D are temperature-dependent empirical coefficients, Z_i and Z_j are the cation and anion charges, respectively. $B_{ij} = B_{1ij} + B_{2ij}T + B_{3ij}T^2$ (where T is the temperature, in Celsius), and the other coefficients C and D have similar forms of temperature dependence. For the activity coefficient of an anion, the subscript i represents that anion and the subscript j then represents all cations in the solution. Each ion pair is described with this nine-parameter equation.

The kinetics of DSP precipitation

The kinetics of DSP precipitation have been widely studied.[21,44–48] Almost all researchers agree that the rate is second order with respect to the degree of silica supersaturation driving force.

$$\frac{dC_{SiO_2}}{dt} = -k_2(C_{SiO_2} - C^*_{SiO_2})^2 \quad (20)$$

In this work, Eq. 20 was also used to fit the experimental data for DSP precipitation. Equation 20 shows that regardless of the mechanism of the formation of DSP, the effect of concentration is very strong. Consequently, accurate knowledge of the equilibrium concentration, C^*_{SiO2}, is essential for the reliable prediction of the degree of supersaturation of the liquor and the rate of DSP deposition. Several correlations have been proposed in the literature for the prediction of silica equilibrium concentration in NaOH-NaAl(OH)$_4$ solution.[31,49–51] In this study, the following expression originally derived by Oku and Yamada[31] was used to calculate silica equilibrium concentration

$$C^*_{SiO_2} = \frac{2.7 \times 10^5 \times M_{Na_2O} \times M_{Al_2O_3}}{MW_{SiO_2}} \quad (21)$$

where M_{Na_2O} and M_{Al_2O3}, respectively, represent Na_2O and Al_2O_3 concentrations (g L^{-1}) of the sodium aluminate solution. MW_{SiO_2} is the molar mass of SiO_2 in g mol^{-1}.

Results and Discussion

Characterization of the original bauxite

The chemical and mineralogical phase compositions of the original bauxite samples were determined by XRF and XRD using quantitative reference intensity rationing phase analysis,[52] respectively. The analysis results are shown in Table 1. As can be seen, more than 60% of the bauxite ore is diaspore. Other phases include ~11% silicon dioxide in the form of kaolinite and 10% quartz, titanium, and iron impurities. The *A/S* of the bauxite is 5.4, which can be identified as low-grade diasporic bauxite.

Silica stability in NaOH-NaAl(OH)$_4$ solution

Figure 4 shows the variation of silica concentration as a function of time and Al_2O_3 concentration for sodium aluminate solution initially containing 10 g L^{-1} SiO_2 at 90°C. As can be seen, the rate of DSP precipitation decreases rapidly with increasing concentration of Al_2O_3 in solution, indicating the enhanced stability of silica. The composition of DSP precipitated in different concentrations was qualitative sodalite ($3[Na_2O \cdot Al_2O_3 \cdot 2SiO_2] \cdot 2NaOH \cdot 2H_2O$), identified by XRD (Figure 5). So, the DSP precipitation reaction can be expressed by Eq. 2.

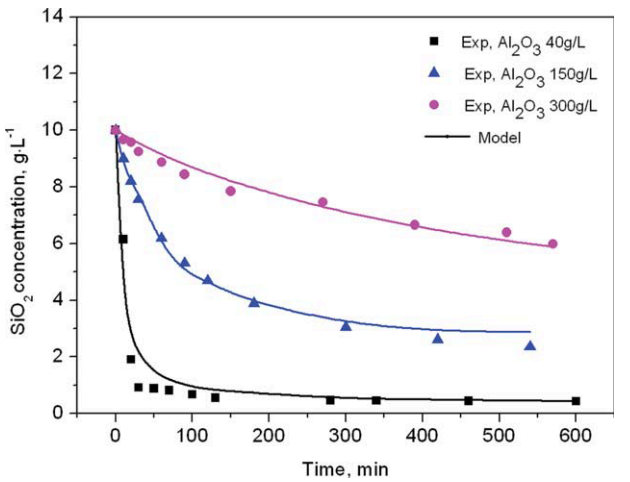

Figure 4. Silica concentration as a function of Al_2O_3 concentration and desilication time in sodium aluminate solution initially containing 400 g L^{-1} NaOH at 90°C.

[Color figure can be viewed in the online issue, which is available at wileyonlinelibrary.com.]

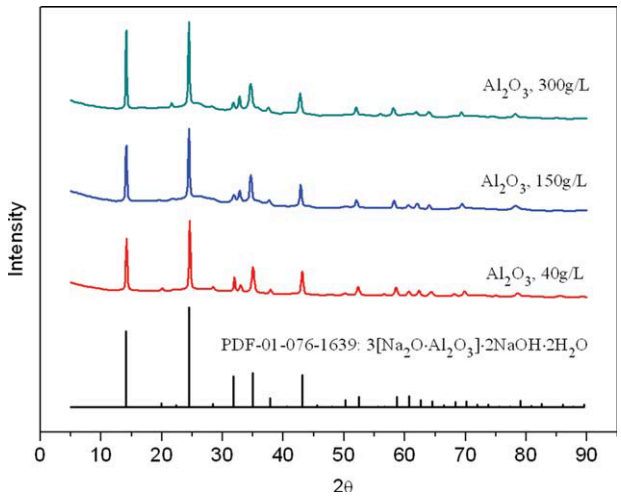

Figure 5. XRD patterns of DSP obtained in sodium aluminate solution initially containing 400 g L^{-1} NaOH at 90°C.

[Color figure can be viewed in the online issue, which is available at wileyonlinelibrary.com.]

Reactive silica leaching in NaOH-NaAl(OH)$_4$ solution

Effect of Leaching Temperature. The influence of temperature on the leaching of reactive silica was investigated, and the results are shown in Figure 6. As can be seen, a similar tendency was observed at all temperatures (80, 90, 100, and 110°C). The silica concentration first increased with leaching time and then decreased sharply with further prolonged leaching time. This means that the silica dissolved from the raw bauxite is not stable and readily precipitates from the liquor as DSP. In addition, the rate of reactive silica dissolution was promoted with the increase of leaching temperature ranging from 80 to 110°C. With the progress of leaching, the rate of DSP formation at high temperature was greater than that at low temperature. One of the possible reasons is that at high leaching temperature, the SiO_2 concentration reached the critical supersaturation threshold more quickly and formed DSP seed, which promoted the rate of DSP precipitation.

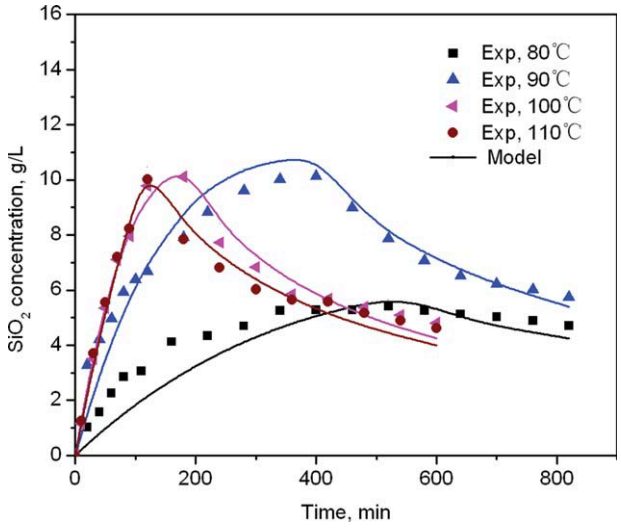

Figure 6. Effect of leaching temperature on the leaching of reactive silica in pure NaOH solution (NaOH 400 g L^{-1}; the particle size 74~98 μm; solid/liquid ratio 0.2).

[Color figure can be viewed in the online issue, which is available at wileyonlinelibrary.com.]

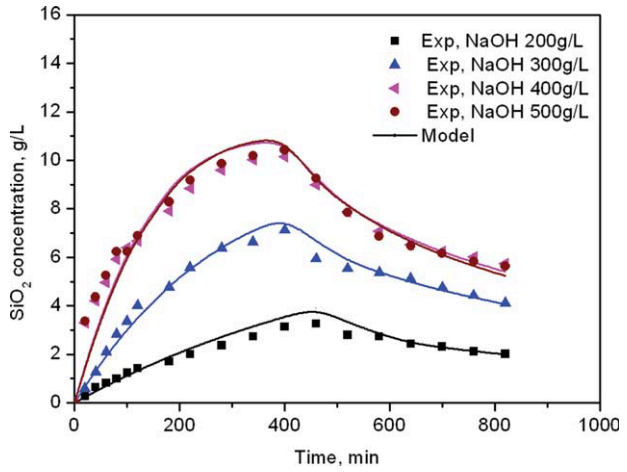

Figure 7. Effect of NaOH concentration on the leaching of reactive silica in pure NaOH solution at 90°C (the particle size 74~98 μm; solid/liquid ratio 0.2).

[Color figure can be viewed in the online issue, which is available at wileyonlinelibrary.com.]

Effect of NaOH Concentration. Figure 7 shows the influence of NaOH concentration on the leaching of reactive silica at 90°C. As can be seen, the silica concentration first increased with leaching time and then decreased rapidly with further prolonged leaching time. Silica reaction with caustic solution involves reactive silica dissolution and DSP precipitation, as shown in Eqs. 1 and 2. At the beginning of leaching, the NaOH concentration is at its highest level, but the concentration of silica is at its lowest. This is interpreted to imply that during the initial stage only dissolution occurs, leading to build-up of silica in the liquor. After a certain time, the build up of silica reaches a critical supersaturation level and precipitation starts, leading to a decrease in dissolved silica content.

Effect of Al_2O_3 Concentration. The effect of Al_2O_3 concentration on the leaching of reactive silica at 90°C was

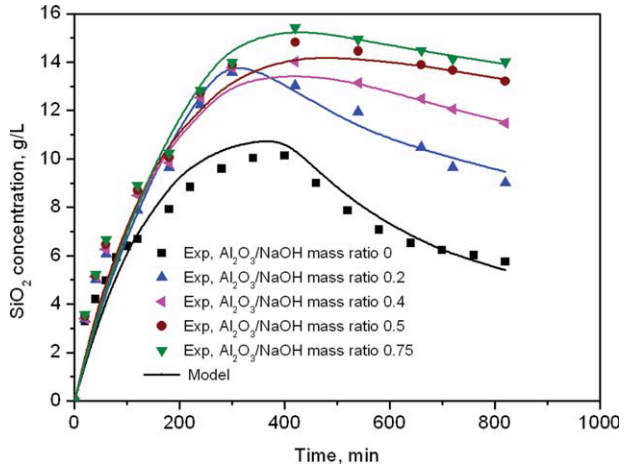

Figure 8. Effect of Al_2O_3 concentration on the leaching of reactive silica at 90°C (NaOH 400 g L^{-1}; the particle size 74~98 μm; solid/liquid ratio 0.2).

[Color figure can be viewed in the online issue, which is available at wileyonlinelibrary.com.]

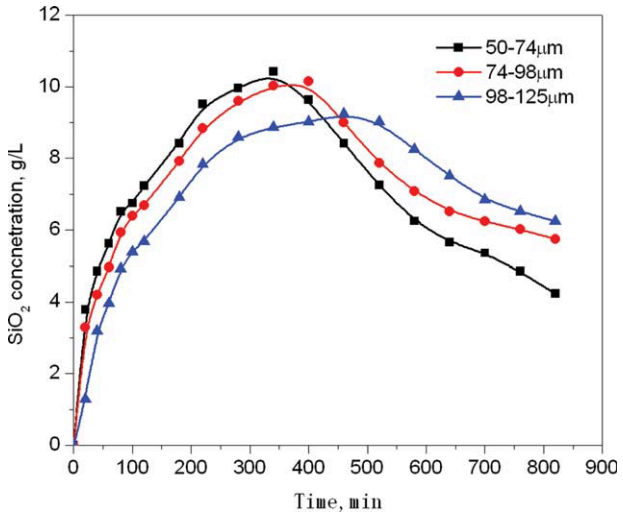

Figure 9. Effect of particle size on the leaching of reactive silica in pure NaOH solution at 90°C (NaOH 400 g L^{-1}; solid/liquid ratio 0.2).

[Color figure can be viewed in the online issue, which is available at wileyonlinelibrary.com.]

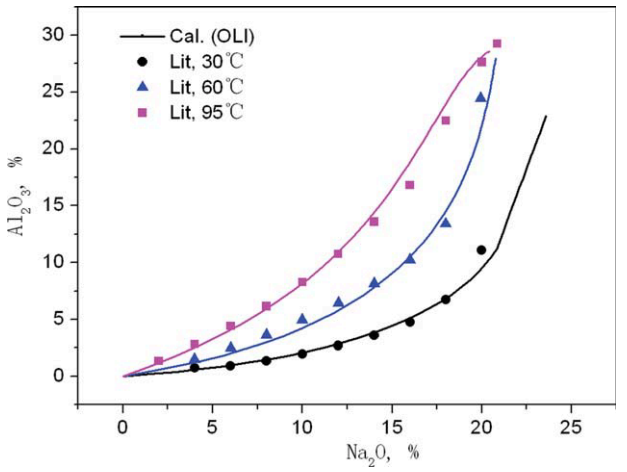

Figure 10. The solubility of gibbsite in NaOH solution.

[Color figure can be viewed in the online issue, which is available at wileyonlinelibrary.com.]

studied, as shown in Figure 8. As can be seen, without the addition of Al_2O_3, the silica concentration reached a very rapid peak and equally dropped to a low level of silica concentration. In this process, the solution was not sufficiently stable to allow the separation of high silica liquor from residual solids. When the concentration of Al_2O_3 was 80 g L^{-1}, silica concentration increased continuously over about 5 h, reaching a maximum silica concentration of 13 g L^{-1}, and then decreased due to the precipitation of DSP. With further increasing of Al_2O_3 concentration to 300 g L^{-1}, the silica concentration reached a maximum of about 15 g L^{-1}, which represents ~65% of the silica content of the bauxite sample, and then decreased smoothly because of DSP precipitation. However, high levels of silica were still maintained for greater than 2 h. This indicted that the liquor of the high alumina and caustic concentrations would suppress DSP precipitation.

Effect of Particle Size. To investigate the effect of the particle size of raw bauxite on the leaching of reactive silica at 90°C, three particle sizes, 50–74 μm, 74–98 μm, and 98–125 μm, were obtained by hierarchical sieving. The results are shown in Figure 9. The particle size was found to have notable effect on silica dissolution. The reason is that the smaller particle size promoted dissolution of reactive silica from the diaspore bauxite, thus reaching the critical supersaturation level more quickly and triggering the precipitation of DSP.

Characterization of the treated bauxite

The residue obtained after leaching at 90°C, NaOH concentration 400 g L^{-1}, Al_2O_3 concentration 300 g L^{-1}, the particle size 74~98 μm, and solid/liquid ratio 0.2, was analyzed. The chemical composition of the treated bauxite sample was determined by XRF, and the analysis results are listed in Table 2. When compared with the chemical composition of the original bauxite (Table 1), the content of SiO_2 in the treated bauxite sample was reduced sharply by reactive silica removal. Up to 65% of silica in the diasporic bauxite was removed into the liquor so that the *A/S* of the diasporic bauxite was enhanced from 5.4 to 15. So, the upgrading of diaspore bauxite was fulfilled by reactive silica removal in concentrated NaOH-$NaAl(OH)_4$ solution at atmospheric pressure. The mineralogical phases of the treated bauxite were identified by the polarizing microscope and were mainly diaspore and secondary hematite, kaolinite, and quartz. The results of the polarizing microscope analysis indicated that the reactive silica in the form of kaolinite was removed from the original bauxite into the concentrated NaOH-$NaAl(OH)_4$ solution. Furthermore, it was found that quartz present in the raw bauxite was not readily attacked by alkali solution at low temperature. Finally, a small quantity of kaolinite remaining in the treated bauxite was noted to be associated with hematite.

Table 2. The Chemical Composition of the Treated Bauxite, Red Mud, and Product Al_2O_3 Obtained in This Study

	Composition (wt. %)					
Material source	Al	Si	Fe	Ti	Ca	Na
Treated bauxite	37.43	2.17	4.44	2.72	0.16	0.55
Red mud	11.97	9.48	8.09	4.55	14.02	3.78
Product Al_2O_3	52.31	0.009	0.014			0.38

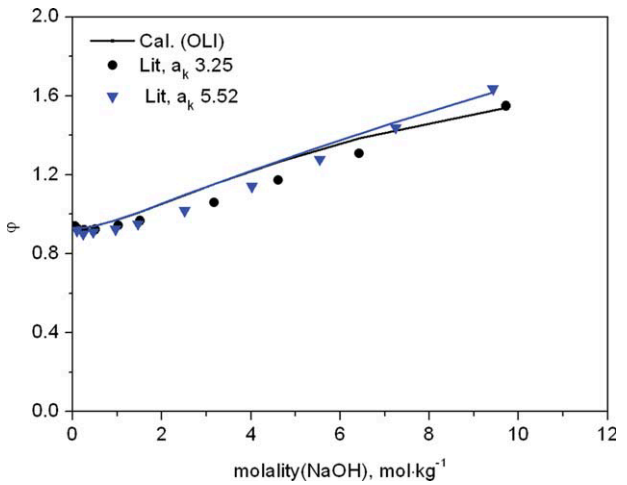

Figure 11. The osmotic coefficients for the NaOH-$NaAl(OH)_4$-H_2O system at 313.2 K and 0.1 Mpa.

[Color figure can be viewed in the online issue, which is available at wileyonlinelibrary.com.]

Table 3. The Model Parameters of the Leaching Process of Reactive Silica at Different Temperatures

Leaching temperature (°C)	k_1 (kg L^{-1} min^{-1})	k_2 (L mol^{-1} min^{-1})
80	3.15×10^{-5}	0.0053
90	1.47×10^{-4}	0.0126
100	2.65×10^{-4}	0.02
110	5.24×10^{-4}	0.0256

Table 4. The Model Parameters of the Leaching Process of Reactive Silica at Different NaOH Concentrations

NaOH Concentration (g L^{-1})	k_1 (kg L^{-1} min^{-1})	k_2 (L mol^{-1} min^{-1})
200	6.63×10^{-5}	0.0118
300	0.95×10^{-4}	0.0122
400	1.47×10^{-4}	0.0126
500	1.72×10^{-4}	0.0127

The model

Validation of OLI's Calculation. Previous studies[53–56] demonstrated that the Bromley–Zemaits activity coefficient model embedded in OLI platform has been successfully applied for predicting or calculating works in acidic media or alkaline solutions. Likewise, the Bromley–Zemaits activity coefficient model may be applied in calculating the OH^- ion activity coefficient in this study. It is considerably important to evaluate the validity of calculation by OLI software with default parameters. This was done by comparing OLI's prediction in estimating gibbsite solubility in NaOH solutions with the experimental data reported in the literature.[57] Both sets of data (OLI predictions and experiments) are plotted in Figure 10 for the case of the solubility of gibbsite in 0.0−22.0 mol kg^{-1} NaOH solutions at different temperatures. As can be observed, the comparison is satisfactory. Also, to further test the validity of calculation by OLI software, a comparison of calculated values by OLI and experimental data reported in the literature[58] for the case of the osmotic coefficients φ at 313.2 K for the NaOH-NaAl$(OH)_4$-H_2O system with the caustic modulus (α_k, molar ratio of Na_2O to $A1_2O_3$) from 3.25 to 5.52 is presented in Figure 11. As can be seen, OLI gives reasonable calculated values of φ. Therefore, the OH^- ion activity in the NaOH-NaAl$(OH)_4$-H_2O system calculated by the existing OLI model can be used to fit the kinetic data in the next section.

Kinetic Model Parameter and Activation Energy. For the reactive silica dissolution controlling step, a good fit of the model (Eq. 15) to experimental data at different temperatures was observed in Figure 6. The model parameters were obtained by nonlinear regression analysis using the software MATLAB and summarized in Table 3. As can be seen, the dissolution kinetic rate constant (k_1) increases with temperature. The model was also found to be applicable for fitting the experimental data under other operating conditions (see Figures 7 and 8), and the model parameters are summarized in Tables 4 and 5.

Table 5. The Model Parameters of the Leaching Process of Reactive Silica at Different Al_2O_3 Concentrations

Al_2O_3 Concentration (g L^{-1})	k_1 (kg L^{-1} min^{-1})	k_2 (L mol^{-1} min^{-1})
0	1.47×10^{-4}	0.0126
80	1.52×10^{-4}	0.00435
160	1.615×10^{-4}	0.00103
200	1.845×10^{-4}	0.000526
300	2.005×10^{-4}	0.000101

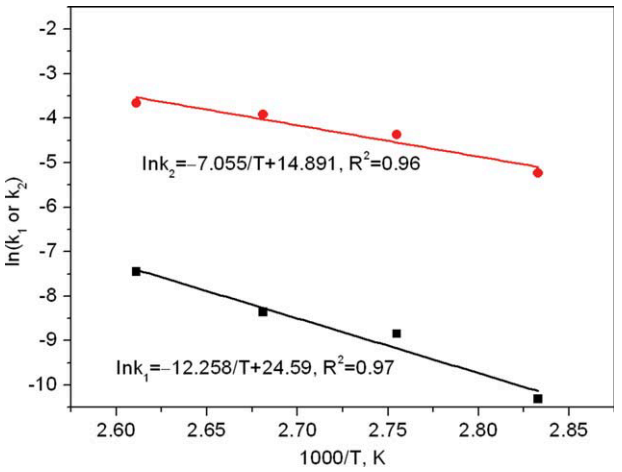

Figure 12. The Arrhenius plots for the leaching kinetics of reactive silica.

[Color figure can be viewed in the online issue, which is available at wileyonlinelibrary.com.]

For determination of the DSP precipitation controlling step, a good agreement of the model (Eq. 20) to experimental data at different temperatures was achieved in the parameter estimation, as shown in Figure 6. The model parameters determined by nonlinear regression analysis are also shown in Table 3. Moreover, the model was also found to be applicable for fitting the experimental data under other operating conditions, as shown in Figures 7 and 8, and the model parameters are also summarized in Tables 4 and 5. In addition, it was found that the model can successfully predict the experimental data of silica stability in NaOH-$NaAl(OH)_4$ solution, as shown in Figure 4.

The slopes of the curves in Figure 6 can be used to determine the apparent reaction rate constants for various temperatures in both reactive silica dissolution and DSP precipitation steps. Then these data obtained were used to draw Arrhenius plots, as shown in Figure 12. The calculated values of the activation energies were 101.91 kJ mol^{-1} for the reactive silica dissolution controlling step and 58.65 kJ mol^{-1} for the DSP precipitation controlling step,

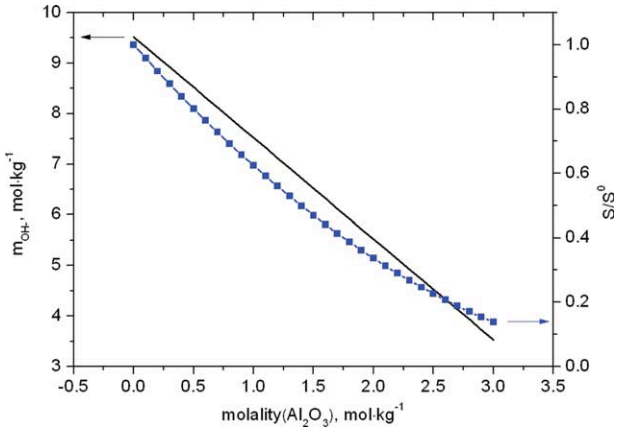

Figure 13. S/S^0 and OH^- ion concentration as a function of Al_2O_3 concentration at 90°C in Na_2O (5 m)-Al_2O_3-SiO_2 (0.25 m)-H_2O system.

[Color figure can be viewed in the online issue, which is available at wileyonlinelibrary.com.]

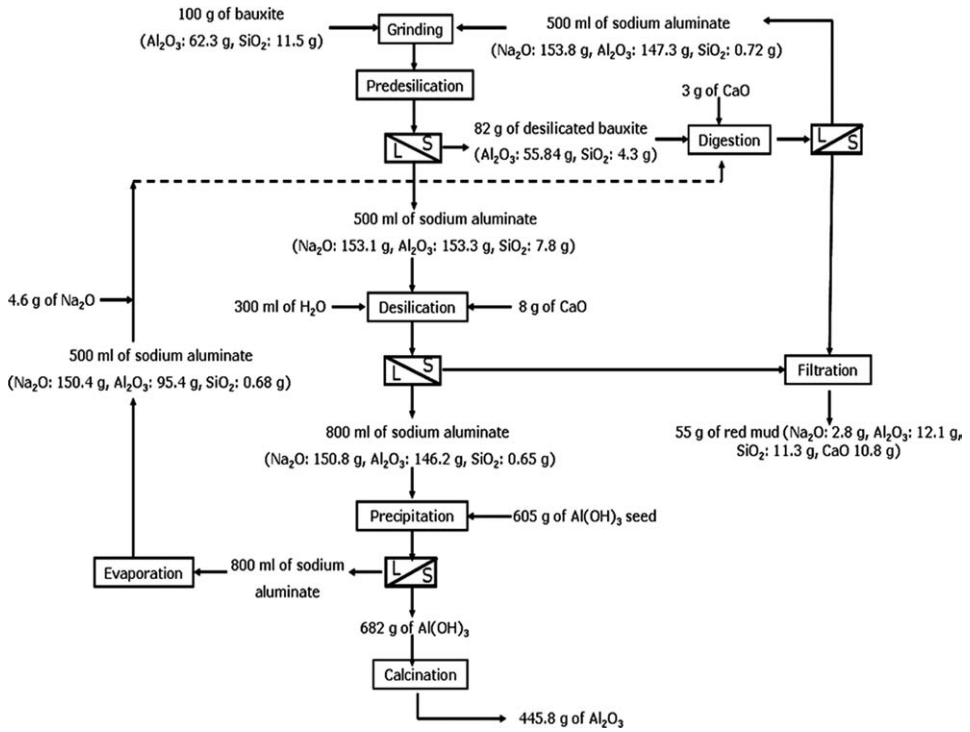

Figure 14. Illustrative flowsheet of the proposed process for low-grade diasporic bauxite treatment.[3]

respectively. Therefore, the reactive silica dissolution and DSP precipitation steps are both limited by chemical reaction.[59]

The mechanism of reactive silica stabilization in concentrated NaOH-NaAl(OH)$_4$ solution

The experimental results mentioned above show that the sodium aluminate solution with high alumina concentration can stabilize a high level of silica in liquor for a period of time sufficient to effect a solid/liquid separation. The mechanism of reactive silica stabilization in concentrated NaOH-$NaAl(OH)_4$ solution can be explained from two perspective. Qualitatively, a probable explanation could be that the dissolved alumina is reacted with the dissolved silica to form Al-Si oligomers,[60–62] as seen in Eq. 22. Al-Si oligomers are soluble so that the dissolved silica can be stabilized for a longer time until the polymerization phenomena occurs,[63,64] as seen in Eq. 23. Eventually, aluminosilicates are precipitated.[65,66]

$$H_2SiO_4^{2-} + 2Al(OH)_4^{2-} \longleftrightarrow [Al_2(H_2SiO_4)(OH)_6]^{2-} + 2OH^- \quad (22)$$

$$(HO)_{4-x}SiO_x^{x-} + Al(OH)_4^- \longleftrightarrow (HO)_3AlOSiO_x(OH)_{3-x}^{(x+1)-} + H_2O \quad (23)$$

Quantitatively, supersaturation of DSP (Eq. 2) can be calculated with the aid of OLI platform according to Eq. 3.

$$8Na^+ + 2OH^- + 6Al^{3+} + 6SiO_2(aq) + 14H_2O \longleftrightarrow Na_8Si_6Al_6O_{24}(OH)_2(H_2O)_2(s) + 24H^+ \quad (2)$$

The K_{sp} of DSP is unavailable because the composition of DSP is very complicated. Therefore, the relative supersaturation (S/S^0) for the DSP-NaOH-$NaAl(OH)_4$-H_2O system was expressed in the form of Eq. 24 and calculated by ignoring the changes of a_{Na^+}, $a_{Al^{3+}}$, $a_{SiO_2(aq)}$, a_{H^+}, and γ_{OH^-} in solutions with various Al_2O_3 concentrations.

$$\frac{S}{S^0} \approx \left(\frac{m_{OH^-}}{m_{OH^-}^0}\right)^2 \quad (24)$$

where S^0 and m_{OH}-^{0}, respectively, represent the supersaturation and OH^- concentration (mol kg^{-1}) in pure NaOH solution.

Figure 13 shows the $S/S^0$and OH^- ion concentration in the Na_2O (5 m)-Al_2O_3-SiO_2 (0.25 m)-H_2O system, as a function of Al_2O_3 concentration. It can be observed that the concentration of OH^- ion decreases sharply due to the formation of

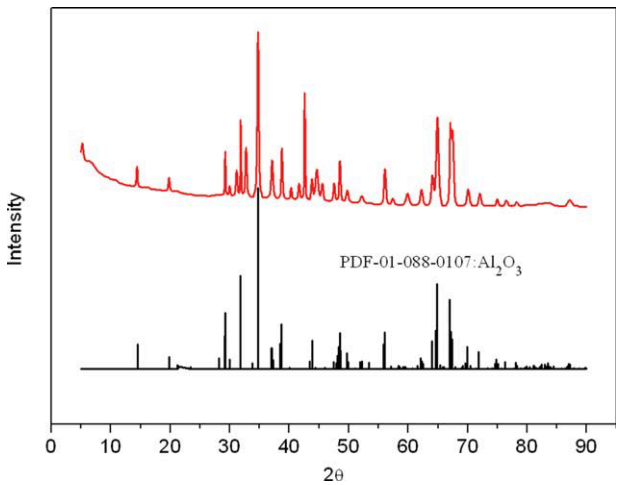

Figure 15. XRD pattern of Al_2O_3 obtained in this study.

[Color figure can be viewed in the online issue, which is available at wileyonlinelibrary.com.]

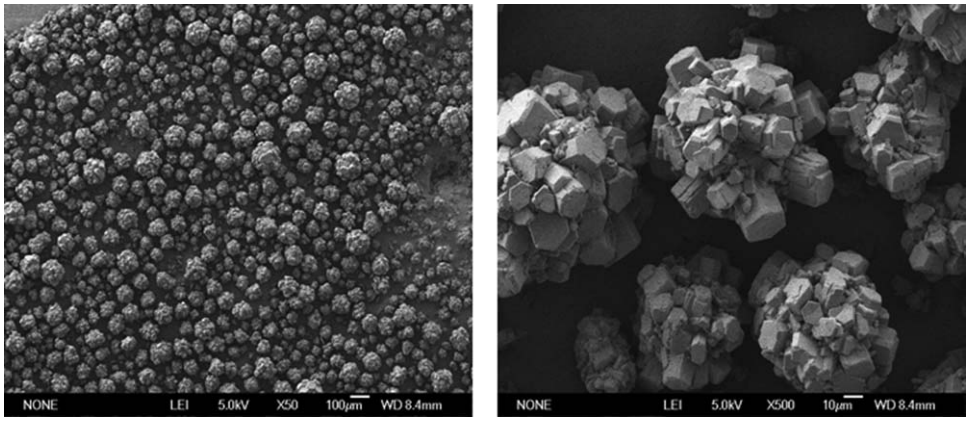

Figure 16. SEM morphologies of Al_2O_3 obtained in this study.

$Al(OH)_4^-$ species with increasing Al_2O_3 concentration. As a result, the supersaturation of DSP decreases sharply (Figure 13), indicating that DSP precipitation is greatly suppressed. This is consistent with the experimental results of silica stability, as shown in Figure 4.

Development of a new process for Al_2O_3 production from low-grade diasporic bauxite

On the basis of the theoretical analysis and experimental results mentioned above, a predesilication operation is introduced into the traditional Bayer process. As a result, a new process for Al_2O_3 production from low-grade diasporic bauxite based on reactive silica dissolution and stabilization in NaOH-$NaAl(OH)_4$ solutions is generated, as shown in Figure 14.

The new process includes the key steps of leaching of reactive silica into sodium aluminate solution, desilication of sodium aluminate solution with high silica content, gibbsite precipitation, followed by calcination of the gibbsite to alumina (Al_2O_3) and digestion of the desilicated bauxite into hot caustic solution. Al_2O_3 production through this new process was successfully tested in the laboratory.

Based on the experimental results, the mass balances for the main constituents such as SiO_2, Al_2O_3, and Na_2O of the proposed process were obtained, as also shown in Figure 14. Moreover, continuous and fully instrumented experiments were carried out and similar results were obtained. The Al_2O_3 product obtained from the continuous experiments was analyzed by XRD, SEM, and XRF, and the results are shown in Figures 15 and 16 and Table 2, respectively. As can be seen, the final product Al_2O_3 crystallizes well with a size of around 80 μm and meets the specifications of metallurgical grade alumina.[1] In addition, the red mud obtained was analyzed using XRF, and the results are also given in Table 2. It shows that the *A*/*S* of the red mud is $\sim$1.2, indicating a high Al_2O_3 recovery from this new process.

Conclusions

A new process of Al_2O_3 production from low-grade diasporic bauxite based on reactive silica dissolution and stabilization in concentrated NaOH-$NaAl(OH)_4$ solution is proposed and proven feasible by the experiments and models shown in this work.

- Different parameters such as NaOH concentration, mean particle size of the diasporic bauxite, Al_2O_3 concentration, leaching temperature, and time influence reactive silica leaching in NaOH-$NaAl(OH)_4$ media. Among them, NaOH and Al_2O_3 concentrations and leaching temperature are the most important determining factors. The optimum condition for reactive silica leaching is at temperature 90°C, NaOH concentration (400 g L^{-1}), particle size (74$\sim$98 μm), Al_2O_3 concentration (300 g L^{-1}), and solid/liquid ratio (0.2). Under the optimum condition, the silica in the diasporic bauxite used herein was removed into the liquor by 65%, which subsequently enhanced the A/S of the bauxite from 5.4 to 15.
- The leaching of reactive silica in NaOH- $NaAl(OH)_4$ media is a typical process of solid–liquid reaction. A classical shrinking core model based on activity for the reactive silica dissolution controlling step and an empirical kinetic model for the controlling step of DSP precipitation have been developed and successfully modeled. The activation energies over the temperature range of 80−110°C were 101.91 and 58.65 kJ mol^{-1} for the two steps, respectively. These values indicate the whole reactive silica leaching process is chemical reaction-controlled.
- In the leaching process of reactive silica, due to the formation of $Al(OH)_4^-$ species, the concentration of OH^- ion and supersaturation in system decrease rapidly with increasing Al_2O_3 concentration of sodium aluminate solution. As a result, DSP precipitation was suppressed greatly. Therefore, a high caustic and alumina concentration in the liquor can allow rapid solubilization of reactive silica and stabilize a high level of silica in solution for a period of time sufficient to effect a solid/liquid separation.
- The proposed process was successfully tested in a continuous loop. The product of Al_2O_3 obtained meets the specifications of the metallurgical grade alumina. Hence, the new process paves the way for Al_2O_3 production from low-grade diasporic bauxite with high reactive silica content.

Acknowledgments

The authors gratefully acknowledge the financial support of National Natural Science Foundation of China (Grant No. 21076212) and National Basic Research Program of China (973 Program, 2007CB613501, 2009CB219904).

Notation

A/S = mass ratio of Al_2O_3/SiO_2
DSP = desilication products
S = supersaturation
K_{sp} = the solubility product constant of DSP
k = the kinetic rate constant (refer to Eq. 10)
k_1 = the dissolution kinetic rate constant of reactive silica, kg L^{-1} min^{-1}

k_2 = the precipitation kinetic rate constant, L mol^{-1} min^{-1}
t = leaching time, min
A = the surface area of the particles
N = the number of particles
C_i, C_i^* = concentration at any time and at equilibrium of the species i, mol L^{-1}
MW_i = the molar mass of the species i, g mol^{-1}
C_i^0 = the initial concentration of the species i, mol L^{-1}
m_i = the molality of the species i, mol kg^{-1}
M_{Na_2O} = Na_2O concentration of sodium aluminate solution, g L^{-1}
M_{Al_2O3} = Al_2O_3 concentration of sodium aluminate solution, g L^{-1}
α_k = molar ratio of Na_2O to $A1_2O_3$

Greek letters

α_i = activity of the species i, mol kg^{-1}
γ_i = activity coefficient of the species i
γ = the average particle radius
γ_0 = the initial particle radius
ρ = the solution density, g·mL^{-1}
φ = the osmotic coefficients for the NaOH-$NaAl(OH)_4$-H_2O system

Literature Cited

1. Burkin AR. *Production of Aluminium and Alumina*. New Jersey: Wiley, 1987.
2. Smith P. The processing of high silica bauxites-review of existing and potential processes. *Hydrometallurgy*. 2009;98:162–176.
3. Hollitt MJ, Crisp AJ, Staker WS, Roe GM, Rodda P. Process for removing reactive silica from a Bayer process. U.S. Patent 6,309,615-B1, 1999.
4. Huang CB, Wang YH. Removal of aluminosilicates from diasporic-bauxite by selective flocculation using sodium polyacrylate. *Sep Purif Technol*. 2008;59:299–303.
5. Papanastassiou B, Csoke B, Solymar K. *Improved preparation of the Greek diasporic bauxite for Bayer-process*. In: Schneider WA, editor. *Light Metals 2002*. Warrendale, PA: The Minerals, Metals & Materials Society (TMS), 2002: 67–74.
6. Ma C, Tian XW, Liu RD, Yang XF. *Selection of Bayer digestion technology and equipment for Chinese bauxite*. In: Hale W, editor. *Light Metals 1996*. Warrendale, PA: The Minerals, Metals & Materials Society (TMS), 1996: 187–191.
7. Jiang TL, Li GF, Huang CB, Fan X, Qiu GR. *Thermal behaviors of kaolinite-diasporic bauxite and desilication from it by roasting-alkali leaching processing*. In: Wolfgang A, Schneider, editors. *Light Metals 2002*. Warrendale, PA: The Minerals, Metals & Materials Society (TMS), 2002:89–94.
8. Chen W, Peng G. *The Digestion Technology of Diasporic Bauxite*. Beijing: Metallurgical Industry Press, 1997.
9. Hu YH, Wang YH, Wang DZ. *Flotation Chemistry of Aluminum and Silicate and Desilication of Bauxite*. Beijing: Science Press, 2004.
10. Li W, Hou P, Wang S. *A new process technology of bauxite concentration-tube digestion for alumina production*. In: Wolfgang A, Schneider, editors. *Light Metals 2002*. Warrendale, PA: The Minerals, Metals & Materials Society (TMS), 2002: 95–100.
11. Hu Y, Jiang H, Qiu G. Solution chemistry of flotation separation of diasporic bauxite. *Chin J Nonferrous Met*. 2001;1:125–130.
12. Massola CP, Chaves AP, Lima JRB, Andrade CF. Separation of silica from bauxite via froth flotation. *Miner Eng*. 2009;22:315–318.
13. Gu S, Yin Z, Qi L. *Intensifying method of Bayer digestion process of diasporic bauxite in China*. In: Wolfgang A, Schneider, editors. *Light Metals 2002*. Warrendale, PA: The Minerals, Metals & Materials Society (TMS), 2002: 83–88.
14. Zhao H. *Digestion of diasporic bauxite with mass ratio of Al2O3/SiO2 no greater than 7 by Bayer process with an excessive addition of lime*. In: Wolfgang A,Schneider, editors. *Light Metals 2002*. Warrendale, PA: TMS, 2002:101–104.
15. Solymar K, Steiner J, Zoldi J. *Technical peculiarities and viability hydrothermal treatment of red mud*. In: Huglen R, editor. *Light Metals 1997*. Warrendale, PA: The Minerals, Metals & Materials Society (TMS), 1997: 49–54.
16. Boros J, Csillag Z, Ferenczi T. Catalyst for bauxite digestion-for the conversion of goethite and hematite. U.S. Pat. No. 4,226,838-A, 1978.
17. Liu WC, Yang JK, Xiao B. Review on treatment and utilization of bauxite residues in China. *Int J Miner Process*. 2009;93:220–231.
18. Ma SH, Wen ZG, Chen JL, Zheng SL. An environmentally friendly design for low-grade diasporic-bauxite processing. *Miner Eng*. 2009;22:793–798.
19. Ni LP. A study of hydrogarnets formed in the Al_2O_3-CaO-Fe_2O_3-Na_2O-SiO_2-H_2O system. *Russ J Inorg Chem*. 1968;13:1585–1587.
20. Tizon E, Clerin P, Cristol B. *Effect of predesilication and digestion conditions on silica level in Bayer liquor*. In: Alton T,Taberaux, editors. *Light Metals 2004*. Warrendale, PA: The Minerals, Metals & Materials Society (TMS), 2004: 9–14.
21. Cousineau PG, Fulforf GD. *Aspect of the desilication of Bayer liquor*. In: Zabreznik, editor. *Light Metals 1987*. Warrendale, PA: The Minerals, Metals & Materials Society (TMS), 1987: 11–17.
22. Grubbs DK. *Reduction of fixed soda losses in the Bayer process by low temperature processing of high silica bauxites*. In: Zabreznik, editor. *Light Metals 1987*. Warrendale, PA: The Minerals, Metals & Materials Society (TMS), 1987: 19–25.
23. Baksa G, Vallo F, Sitkei F, Zoldi J, Solymar K. *Complex causticisation: an effective means for the reducing of NaOH losses in an alumina plant*. In: Miller RE, editor. *Light Metals 1986*. Warrendale, PA: The Minerals, Metals & Materials Society (TMS), 1986:75–80.
24. Roberts RC. Method for extraction alumina from its ores. U.S. Patent 3,413,087, 1968.
25. Tizon E, Fryns C. The Bayer process for production of alumina trihydrate by alkaline digestion of bauxite, the process comprising a predesilication step. U.S. Patent 2007–0,178,041-A1, 2007.
26. Jamialahmadi M, Müller-Steinhagen H. Determining silica solubility in Bayer process liquor. *JOM*. 1998;50:44–49.
27. Roach GID, White AJ. *Dissolution kinetics of kaolin in caustic liquors*. In: Boxall LG, editor. *Light Metals 1988*. Warrendale, PA: The Minerals, Metals & Materials Society (TMS), 1987: 41–47.
28. Banvolghi G, Toth AC, Tasst I. *In-situ formation of sodium aluminum hydrosilicate from kaolinite*. In: Rooy E, editor. *Light Metals 1991*. Warrendale, PA: The Minerals, Metals & Materials Society (TMS), 1991:5–15.
29. Wen QG. A FTIR study of dissolution and precipitation of silica in Bayer process. *J Wuhan Univ Technol*. 1997;1–2:1–8.
30. Buhl JC, Buckermann W, Hoffmann W, Muller-Warmuth W. The crystallization kinetics of sodalites grown by the hydrothermal transformation of kaolinite as studied by Si MAS NRM. *Solid State Nucl Magn Reson*. 1997;9:121–128.
31. Oku T, Yamada K. *The dissolution rate of quartz and the rate of desilication in the Bayer process*. In: Nuttall K, editor. *Light Metals 1971*. Warrendale, PA: The Minerals, Metals & Materials Society (TMS), 1971:31–45.
32. Bickmore BR, Nagy KL, Gray AK, Brinkerhoff AR. The effect of on the dissolution rate of quartz. *Geochim Cosmochim Acta*. 2006;70:290–305.
33. Barcza L, Palfalvi-Rozsahegyi M. The aluminate lye as a system of equilibria. *Mat Chem Phys*. 1989;21:345–356.
34. Lippincott ER, Psellos JE, Tobin MC. The Raman spectra and structures of aluminate and zincate ions. *J Chem Phys*. 1952;20:536.
35. Mal'tsev GZ, Malinin GV, Mashovets VP, Shcherbakov VA. Thermodynamic properties and H^1 and Na^{23} NMR spectra of sodium hydroxide solutions. *Russ J Struct Chem*. 1965;6:353–358.
36. Moolenaar RJ, Evans JC, McKeever LD. The structure of the aluminate ion in solutions at high PH. *J Phys Chem*. 1970;74:3629–3636.
37. Panias D, Asimidis P, Paspaliaris I. Solubility of boehmite in concentrated sodium hydroxide solutions: model development and assessment. *Hydrometallurgy*. 2001;59:15–29.
38. Croker D, Loan M, Hodnett BK. Desilication reaction at digestion conditions: an in situ X-ray diffraction study. *Cryst Growth Des*. 2008;8:4499–4505.
39. Levenspiel O. *Chemical Reaction Engineering*, 2nd ed. New York: Wiley, 1972.
40. Raghavan NS, Fulford GD. *Mathematic modeling of the kinetics of gibbsite and kaolinite dissolution/desilication in the Bayer process*. In: Sahoo M,Fradet C, editors. *Light Metals 1998*. Warrendale, PA: The Minerals, Metals & Materials Society (TMS), 1998:29–36.
41. Zemaitis JF. *Predicting vapor-liquid-solid equilibria in multicomponent aqueous solutions of electrolytes*. In: Newman SA,Barner HE,Klein M, editors. *Thermodynamics of Aqueous Systems with Industrial Applications. ACS Symposium Series 133*; Washington, DC: American Chemical Society, 1980: 227–246.
42. Rafal M, Berthold JW, Scrivner NC, Grise SL. Models for electrolyte solutions. In,: Sandler SIeditor. *Models for Thermodynamic and Phase Equilibria Calculations*. New York: Marcel Dekker, 1994.

43. Bromley LA. Thermodynamic properties of strong electrolytes in aqueous solutions. *AIChE J*. 1973;19:313–320.
44. Ma JY, Zhai KM, Li ZB. Desilication of synthetic Bayer liquor with calcium sulfate dihydrate: kinetics and modelling. *Hydrometallurgy*. 2011;107:48–55.
45. Barnes MC, Addai-Mensah J, Gerson AR. The kinetics of desilication of synthetic Bayer liquor seeded with cancrinite and cancrinite/sodalite mixed-phase. *J Cryst Growth*. 1999;200:251–264.
46. Barnes MC, Addai-Mensah J, Gerson AR. The kinetics of desilication of synthetic spent Bayer liquor and sodalite crystal growth. *Colloids Surf A*. 1999;147:283–295.
47. Müller-Steinhagen H, Jamialahmadi M, Robson B. Understanding and mitigating heat exchanger fouling in bauxite refineries. *JOM*. 1994;46:36–41.
48. O'Neill GA. *Prediction of heat exchanger heat transfer coefficient decay due to fouling*. In: Miller RE, editor. *Light Metals 1986*. Warrendale, PA: The Minerals, Metals & Materials Society (TMS), 1986:133–140.
49. Adamson AN, Bloore EJ, Carr AR. Basic principles of Bayer process design. *J Extr Met Aluminum*. 1963;1:23–58.
50. Cresswell PJ. Factors affecting desilication of Bayer process liquor. *CHEMECA*. 1984;48:285–292.
51. Leiteizen MG. Kinetics of converting bauxite silica to sodium aluminosilicate. *TSV Met*. 1972;45:37–40.
52. Solymar K, Sajo I, Steiner J, Zoldi J. *Characteristics and separability of red mud*. In: Cutshall ER, editor. *Light Metals 1992*. Warrendale, PA: The Minerals, Metals & Materials Society (TMS), 1992:209–223.
53. Li ZB, Demopoulos GP. Development of an improved chemical model for the estimation of CaSO4 solubilities in the HCl-CaCl2-H2O system up to 100 °C. *Ind Eng Chem Res*. 2006;45:2914–2922.
54. Li ZB, Demopoulos GP. Speciation-based chemical model of CaSO4 solubility in the H+Na+Ca+Mg+Al+ Fe(II) +Cl+SO4+H2O system. *Ind Eng Chem Res*. 2007;46:6385–6392.
55. Cheng WT, Li ZB. Controlled supersaturation precipitation of hydromagnesite for the MgCl2-Na2CO3 system at elevated temperatures: chemical modelling and experiment. *Ind Eng Chem Res*. 2010;49:1964–1974.
56. Ma JY, Li ZB. Chemical equilibrium modeling and experimental measurement of solubility for Friedel's salt in the Na-OH-Cl-NO3-H2O systems up to 200 °C. *Ind Eng Chem Res*. 2010;49:8949–8958.
57. Russell AH, Edwards JD, Taylor CS. Solubility of hydrated aluminas in NaOH solutions. *J Met*. 1955;203:1123–1128.
58. Zhou J, Chen QY, Li J, Yin ZL, Zhou X, Zhang PM. Isopiestic measurement of the osmotic and activity coefficients for NaOH-NaAl(OH)4-H2O system at 313.2K. *Geochim Cosmochim Acta*. 2003;67:3459–3472.
59. Habashi F. *Principles of extractive metallurgy, Vol. 1*. New York: Gordon and Breach, 1969.
60. Iler RK. *The Chemistry of Silica: Solubility, Polymerization, Colloid and Surface Properties, and Biochemistry*. New York: Wiley, 1979.
61. Hanzlicek T, Steinenova-Vondrakova M. Investigation of dissolution of aluminosilicates in aqueous alkaline solution under laboratory conditions. *Ceram Silik*. 2002;46:97–103.
62. Swaddle TW. Silicate complexes of aluminum (III) in aqueous systems. *Coord Chem Rev*. 2001;219–221:665–686.
63. Dent Glasser LS, Harvey G. The unexpected behaviour of potassium aluminosilicate solutions. *J Chem Soc Chem Commun*. 1984;664–665.
64. Dent Glasser LS, Harvey G. The gelation of behaviour of aluminosilicate solutions containing Na+, K+, Cs+, and MeN+. *J Chem Soc Chem Commun*. 1984;1250–1252.
65. Breck DW. *Zeolite Molecular Sieves*. New York: Interscience, 1974.
66. Chang HL, Shih WH. A general method for the conversion of fly ash into zeolities as ion exchangers for cesium. *Ind Eng Chem Res*. 1998;37:71–78.

Manuscript received Jan. 22, 2011, revision received Mar. 27, 2011, and final revision received Jun. 29, 2011.